

Spectroscopic–kinetic analysis of first and second order reactions on the basis of multidimensional absorbance (A) diagrams

J. Polster and H. Dithmar

Department für Biowissenschaftliche Grundlagen, Lehrstuhl für Biologische Chemie, Technische Universität München, D-85350 Freising-Weihenstephan, Germany

Received 24th July 2000, Accepted 15th January 2001

First published as an Advance Article on the web 28th February 2001

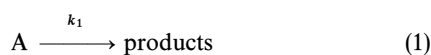
The absorbance (A), absorbance difference (AD) and absorbance difference quotient (ADQ) diagrams are called Mauser diagrams. Typically, these diagrams represent two-dimensional plots. The so-called Mauser space is multidimensional ($n \geq 2$). The axes of this space are established by the absorbances or absorbance differences of n wavelengths. A reaction system that consists only of one linearly independent reaction step ($s = 1$) leads to a straight line in Mauser space. This line is obtained independent of the reaction order of the system. A one-dimensional coordinate axis can be established which is orientated in the direction of the straight line lying in the Mauser space ($n > s$). The distances of the individual measured points with regard to the origin of the (one-dimensional) coordinate system can be evaluated kinetically. The procedure is demonstrated using reactions of first and second order ($s = 1$; $n = 4$ and 6). A reaction system described by two linearly independent steps ($s = 2$) leads to a curve in the Mauser space which lies on a plane. A two-dimensional coordinate system can be introduced which lies in this plane. The coordinates of the Mauser curve with regard to the established (two-dimensional) coordinate system can be evaluated kinetically. The procedure is shown by evaluating reactions of first and second order ($s = 2$; $n = 3$ and 4). The advantages of geometric analysis of Mauser space are discussed.

1 Introduction

Mauser diagrams are a powerful tool for the spectroscopic–kinetic analysis of reaction systems.^{1–5} The number (s) of linearly independent reaction steps can be determined by means of these diagrams as shown in many examples.^{1,2} In addition to this information being important for each reaction system investigated spectroscopically, the (differential) geometric analysis of the absorbance space (the so-called ‘Mauser space’) opens up new perspectives for kinetic evaluation.^{3–5} Until now only two and three-dimensional Mauser spaces were analyzed geometrically in kinetics. The first results of evaluating multidimensional Mauser spaces are reported here.

2 The problem

The mechanism



represents the simplest reaction of first order ($s = 1$). The following differential absorbance equation is true here^{1,2}

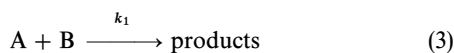
$$dA_\lambda = z_{\lambda 0} dt + z_{\lambda 1} A_\lambda dt \quad (2a)$$

with

$$z_{\lambda 0} = k_1 A_{\lambda \infty} \quad \text{and} \quad z_{\lambda 1} = -k_1 \quad (2b)$$

A_λ is the absorbance at time t and at wavelength λ . The term $A_{\lambda \infty}$ is the absorbance for $t \rightarrow \infty$. The coefficients $z_{\lambda 0}$ and $z_{\lambda 1}$ are constants that relate to the rate constant k_1 and $A_{\lambda \infty}$ as shown.

The mechanism



represents a simple reaction of second order ($s = 1$). In analogy to eqn. (2)^{1,2}

$$dA_\lambda = z_{\lambda 0} dt + z_{\lambda 1}(A_\lambda - A_{\lambda 0}) dt + z_{\lambda 2}(A_\lambda - A_{\lambda 0})^2 dt \quad (4a)$$

with

$$z_{\lambda 0} = k_1 a_0 b_0 Q_\lambda, \quad z_{\lambda 1} = -k_1(a_0 + b_0)$$

and

$$z_{\lambda 2} = k_1/Q_\lambda \quad (4b)$$

where $A_{\lambda 0}$ is the absorbance at $t \rightarrow 0$ ($A_{\lambda 0} = A_\lambda(t \rightarrow 0)$); a_0 and b_0 are the initial concentrations of A and B. Q_λ is a constant that is a function of the absorbance coefficients $\epsilon_{\lambda i}$ of components and the pathlength of the cuvette.^{1,2}

A linear reaction system consisting of two linearly independent steps ($s = 2$) is represented by the following parallel reactions



It is true here that^{1,2}

$$d\mathbf{A} = \mathbf{z}_0 dt + \mathbf{Z} \mathbf{A} dt \quad (6a)$$

with

$$d\mathbf{A} = \begin{pmatrix} dA_1 \\ dA_2 \end{pmatrix}, \quad \mathbf{z}_0 = \begin{pmatrix} z_{10} \\ z_{20} \end{pmatrix}, \quad \mathbf{Z} = \begin{pmatrix} z_{11} & z_{12} \\ z_{21} & z_{22} \end{pmatrix}$$

and

$$\mathbf{A} = \begin{pmatrix} A_1 \\ A_2 \end{pmatrix} \quad (6b)$$

The determinant D and trace S of Z leads to $k_{1,2}$ according to

$$D = z_{11}z_{22} - z_{12}z_{21} = k_1k_2, \quad (6c)$$

$$S = z_{11} + z_{22} = -(k_1 + k_2) \quad (6d)$$

and

$$k_{1,2} = \frac{S \pm (S^2 - 4D)^{1/2}}{2}. \quad (6e)$$

A_1 and A_2 are the absorbances at wavelength λ_1 and λ_2 ($A_1 = A_{\lambda_1}$, $A_2 = A_{\lambda_2}$).

Finally, the two reactions ($s = 2$) of second order:



obey the equations^{1,6}

$$d\mathbf{A} = z_0 dt + \mathbf{Z}\Delta\mathbf{A} dt + \mathbf{Y}\Delta\mathbf{A}^2 dt \quad (8a)$$

with

$$\begin{aligned} d\mathbf{A} &= \begin{pmatrix} dA_1 \\ dA_2 \end{pmatrix}, \quad z_0 = \begin{pmatrix} z_{10} \\ z_{20} \end{pmatrix}, \quad \mathbf{Z} = \begin{pmatrix} z_{11} & z_{12} \\ z_{21} & z_{22} \end{pmatrix}, \\ \Delta\mathbf{A} &= \begin{pmatrix} \Delta A_1 \\ \Delta A_2 \end{pmatrix}, \quad \mathbf{Y} = \begin{pmatrix} y_{11} & y_{12} & y_{13} \\ y_{21} & y_{22} & y_{23} \end{pmatrix}, \\ \Delta\mathbf{A}^2 &= \begin{pmatrix} \Delta A_1^2 \\ \Delta A_2^2 \\ \Delta A_1 \Delta A_2 \end{pmatrix} \end{aligned} \quad (8b)$$

where

$$\Delta A_\lambda = A_\lambda - A_{\lambda 0} \quad (8c)$$

The rate constants k_1 and k_2 for (7a) and (7b) can be calculated by means of the determinant D and trace S of Z as follows

$$D = z_{11}z_{22} - z_{12}z_{21} = k_1k_2 a_0(a_0 + b_0 + e_0) \quad (8d)$$

$$S = z_{11} + z_{22} = -k_1(a_0 + b_0) - k_2(a_0 + e_0) \quad (8e)$$

and

$$k_{1,2} = \frac{-\sigma_1 S \pm [(\sigma_1 S)^2 - 4\sigma_1 \sigma_2 \sigma_3 D]^{1/2}}{2\sigma_1 \sigma_2} \quad (8f)$$

where

$$\sigma_1 = a_0(a_0 + b_0 + e_0) \quad (8g)$$

$$\sigma_2 = a_0 + b_0 \quad (8h)$$

$$\sigma_3 = a_0 + e_0. \quad (8i)$$

$A_{\lambda 0}$ is again the absorbance at $t \rightarrow 0$ ($A_{\lambda 0} = A_\lambda(t \rightarrow 0)$).

The coefficients z_{ij} of eqns. (2a) and (4a) can be determined by formal integration.¹⁻⁶ This is also true for z_{ij} and y_{ij} of z_0 , Z and Y (see eqn. (8a)). The constants z_{ij} lead to the rate constants k_i for the different reaction mechanisms shown by eqns. (2b), (4b), (6e) and (8f).

The accuracy of the kinetic evaluation depends on how spectroscopically perceptibly significant the individual reactions are. When reactions exist which show poorly spectroscopic properties the kinetic evaluation may falter or even fail. This situation may be overcome when several wavelengths (n) that are distributed in the spectra registered are included simultaneously in the evaluation procedure (with $n > s$). However, the differential absorbance equations presented (compare eqns. (2a), (4a), (6a), (8a)) are only true for absorbance values at s wavelengths. The modification of the

presented differential absorbance equations that is true for n wavelengths is shown subsequently. A practical example is given for each reaction mechanism discussed above.

3 Reactions of first and second order consisting of one independent step ($s = 1$)

3.1 Theory

The Mauser space is generated by the absorbance axes of (n) different wavelengths. The absorbances change in dependence on time, leading to a characteristic curve in Mauser space. The absorbances are now represented by a vector \mathbf{A} with the coordinates ($n > s$)

$$\mathbf{A} = \begin{pmatrix} A_{\lambda_1} \\ A_{\lambda_2} \\ \vdots \\ A_{\lambda_n} \end{pmatrix} = \begin{pmatrix} A_1 \\ A_2 \\ \vdots \\ A_n \end{pmatrix} \quad (9)$$

The vector \mathbf{A} is time dependent. Selecting the vector \mathbf{A} for $t \rightarrow 0$, the difference vector $\Delta\mathbf{A}$ can be established according to

$$\begin{aligned} \Delta\mathbf{A} &= \mathbf{A} - \mathbf{A}_0 = \begin{pmatrix} A_1 - A_1(t \rightarrow 0) \\ A_2 - A_2(t \rightarrow 0) \\ \vdots \\ A_n - A_n(t \rightarrow 0) \end{pmatrix} \\ &= \begin{pmatrix} A_1 - A_{10} \\ A_2 - A_{20} \\ \vdots \\ A_n - A_{n0} \end{pmatrix} = \begin{pmatrix} \Delta A_1 \\ \Delta A_2 \\ \vdots \\ \Delta A_n \end{pmatrix} \end{aligned} \quad (10)$$

Each reaction system consisting of one linearly independent reaction (being of first or second order) leads to straight lines in the absorbance (A) and absorbance difference (ΔA) diagrams as shown in refs. 1 and 2. Thus, the ratio of any two ΔA values ($\Delta A_i/\Delta A_j$) in eqn. (10) is a constant

$$\frac{\Delta A_i}{\Delta A_j} = \alpha_{ij} \quad (11)$$

It follows from this fact that a straight line is also obtained in the n -dimensional ΔA or A diagram ($n > s$). The basic law according to Lambert-Beer-Bouguer can be developed for the dependence on concentrations or degrees of advancements (X_i).^{1,2,5,6} In the case of $s = 1$, the general equation (12) is true for reactions of first and second order^{1,2}

$$\Delta A_\lambda = Q_\lambda X_1 \quad (12)$$

where Q_λ is a constant for each wavelength (compare eqn. (4b)). The introduction of eqn. (12) into eqn. (10) leads to

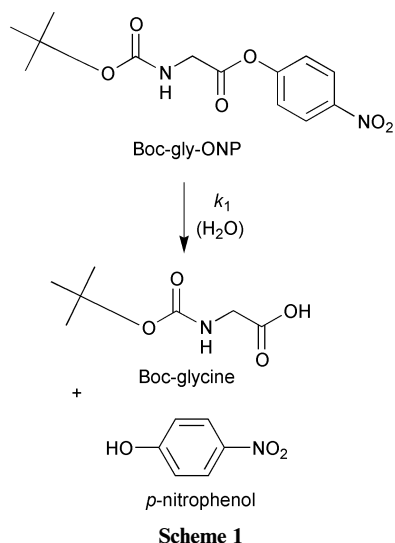
$$\Delta\mathbf{A} = \begin{pmatrix} \Delta A_1 \\ \Delta A_2 \\ \vdots \\ \Delta A_n \end{pmatrix} = \begin{pmatrix} Q_1 \\ Q_2 \\ \vdots \\ Q_n \end{pmatrix} X_1 \quad (13)$$

It follows from this equation that

$$\begin{aligned} \Delta A_1^2 &= Q_1^2 \cdot X_1^2 \\ \Delta A_2^2 &= Q_2^2 \cdot X_1^2 \\ &\vdots \\ \Delta A_n^2 &= Q_n^2 \cdot X_1^2 \end{aligned} \quad (14)$$

Each value of X_1 is dependent on time and so produces a point in the n -dimensional ΔA diagram. The distances v between the origin and these points which lie on a straight line passing through the origin can be computed according to

$$v = [(\Delta A_1)^2 + (\Delta A_2)^2 + \dots + (\Delta A_n)^2]^{1/2} \quad (15)$$



One obtains from eqns. (14) and (15)

$$v = X_1 [Q_1^2 + Q_2^2 + \dots + Q_n^2]^{1/2} \quad (16)$$

Comparison of eqns. (12) and (16) shows that both ΔA_λ and v are proportional to X_1 . However, the factor of proportionality of eqn. (16) is much larger than that of eqn. (12). Thus, an improvement in spectroscopic evaluation should be achieved when the Mauser space is applied.

Instead of eqns. (2a), (2b), (4a) and (4b) it is true here that

$$dv = p_{\lambda 0} dt + p_{\lambda 1} v dt \quad (17a)$$

with

$$p_{\lambda 0} = k_1 v_\infty \quad \text{and} \quad p_{\lambda 1} = -k_1 \quad (17b)$$

and

$$dv = p_{\lambda 0} dt + p_{\lambda 1} v dt + p_{\lambda 2} v^2 dt \quad (18a)$$

with

$$p_{\lambda 0} = k_1 a_0 b_0 Q_v, \quad p_{\lambda 1} = -k_1(a_0 + b_0), \quad p_{\lambda 2} = k_1/Q_v \quad (18b)$$

where v_∞ is the value of v for $t \rightarrow \infty$ and Q_v is a constant (which is not identical with Q_λ). Eqns. (17a) and (17b) can be applied to evaluate linear reactions of rank one ($s = 1$) whereas eqns. (18a) and (18b) are true for second order reactions ($s = 1$).

3.2 Practical examples ($s = 1$)

3.2.1 First order reaction. The spontaneous hydrolysis of Boc-gly-ONP (*N*-*tert*-butoxycarbonylglycine *p*-nitrophenyl

Table 1 Spectroscopic-kinetic analysis of hydrolysis reaction of Boc-gly-ONP (7×10^{-5} M); reaction conditions: 0.1 M borax buffer; pH = 8.7; temperature 25 °C (see ref. 1); evaluation according to eqns. (2a) and (2b). Mean value of k : $2.31 \times 10^{-3} \text{ s}^{-1}$. Evaluation according to eqns. (17a) and (17b) using the four-dimensional Mauser space (A_{420} vs. A_{400} vs. A_{380} vs. A_{290}), $k_1 = 2.31 \times 10^{-3} \text{ s}^{-1}$

λ/nm	420	400	380	290
$k_1 \times 10^3/\text{s}^{-1}$	2.2(9)	2.3(3)	2.3(5)	2.2(6)

ester) has already been studied thoroughly in 0.1 M borax buffer (pH = 8.7, temperature $T = 25.0$ °C).^{1–5} The same reaction (Scheme 1) was used here to test the method presented.

The reaction was spectroscopic-kinetically evaluated at the wavelengths 420, 400, 380 and 290 nm according to routine procedures and according to the new method. The results of evaluation using eqns. (2a) and (2b) are shown in Table 1. As well, the result obtained by eqns. (17a) and (17b) is presented in Table 1. Obviously, nearly an optimal result was achieved here using the four-dimensional Mauser space which contains no time axis. The error in the coefficients could be determined from eqn. (17a) by simulating the curve.^{1,2} This error lay between 0.2 and 1.5% for Scheme 1.

Geometric analysis of the Mauser space is of particular interest in the case of $s > 1$. The geometric properties for the case $s = 2$ discussed subsequently can be understood better when the position of the curve lying in the three-dimensional Mauser space is considered systematically, starting with the case $s = 1$. The absorbances of Scheme 1 lie on a straight line in Fig. 1(a). When the coordinate system is rotated a position can be found where the straight line is regarded as a single point. The ‘size’ of this point gives information about how strongly the points measured are scattered around the straight line observed. According to Fig. 1(b), scattering is weakly pronounced for the reaction shown in Scheme 1. In the case of linear reactions ($s = 1$) the distance v can be related to any point measured (1st, 2nd, ... n th point), meaning that A_0 can be replaced by A_n in eqn. (10) leading to a changed value ΔA and, thus, to an altered value v , (see eqn. (15)).

3.2.2 Second order reaction. The aminolysis of Boc-gly-ONP with *n*-butylamine using the solvent acetonitrile can be described by the second order reaction shown in Scheme 2. The reaction has already been studied in detail and the rate constants were determined using the absorbances at six wavelengths (see Table 2).¹ The kinetic evaluation of the six-dimensional Mauser space leads to a rate constant which lies close to the mean value of the six rate constants obtained at the individual wavelengths (see Table 2). The coefficients of eqn. (18a) showed an error of about 0.4%.

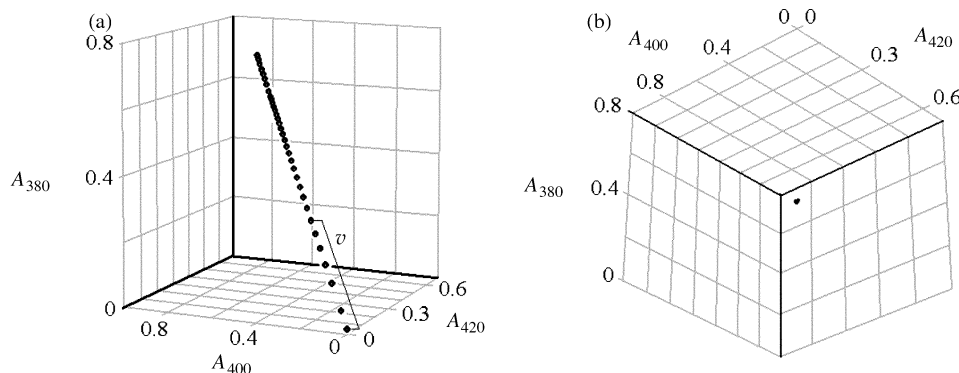
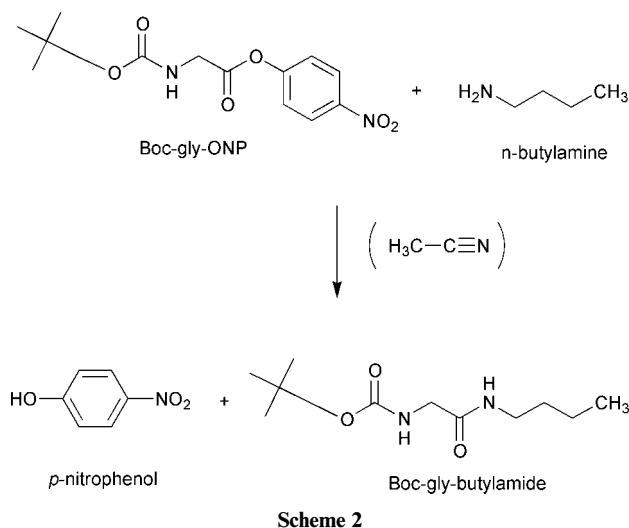


Fig. 1 Three-dimensional A diagrams for Scheme 1 (A_{400} vs. A_{420} vs. A_{380}). The absorbances measured lie on a straight line as shown by part (a). (b) The situation when (a) is rotated until the viewer sees the line as a point. The significance of distance v is shown in part (a).



4 Reactions of first or second order consisting of two independent steps ($s = 2$)

4.1 Theory

Spectroscopically investigated reactions with two independent steps ($s = 2$) of first and/or second order are generally described by means of two degrees of advancement (X_1, X_2) according to^{1,2,5,6}

$$\Delta A_\lambda = A_\lambda - A_{\lambda 0} = Q_{\lambda 1} X_1 + Q_{\lambda 2} X_2 \quad (19)$$

where $A_{\lambda 0} = A_\lambda(t \rightarrow 0)$; $Q_{\lambda 1}$ and $Q_{\lambda 2}$ are constants being dependent on λ .^{1,2}

A typical curve for X_1 vs. X_2 is shown in Fig. 2(a). The curve is starting from the origin P_0 ($t \rightarrow 0$) and is ending at point P_∞ ($t \rightarrow \infty$). A straight line can be constructed which passes through P_0 and P' . P' is a point which can be identical with P_∞ or which lies near P_∞ on the curve with points P ($P' = P$). The line P_0P' generates a new axis which is denoted v' . A second axis, w' , can be introduced which runs perpendicularly to v' and which passes through P_0 (see Fig. 2(a)). Thus, the new coordinate system with axes v' and w' is the result of rotation of the old system with axes X_1 and X_2 . This rotation represents an affine transformation. For example, the eigenvalues (r_1 and r_2) that characterize the curve are preserved during this transformation.

The transduction of Fig. 2(a) into the corresponding two-dimensional absorbance diagram ($A_{\lambda 1}$ vs. $A_{\lambda 2}$) again represents an affine transformation.¹⁻⁵ Thus, the absorbance curve ($A_{\lambda 1}$ vs. $A_{\lambda 2}$) has the same characteristic properties (e.g. the same eigenvalues of Z in eqn. (6a) or eqn. (8a)) as the corresponding curve of X_1 vs. X_2 .¹⁻⁶ This property of preservation is not changed when n -dimensional Mauser diagrams ($A_{\lambda 1}$ vs. $A_{\lambda 2}$ vs. \dots vs. $A_{\lambda n}$) are introduced.

A plot of $A_{\lambda 1}$ vs. $A_{\lambda 2}$ vs. $A_{\lambda 3}$ (shortened to A_1 vs. A_2 vs. A_3) is shown in Fig. 2(b) for $s = 2$. Since, according to eqn. (19), each value A_λ depends on only two variables (X_1, X_2) a curve is

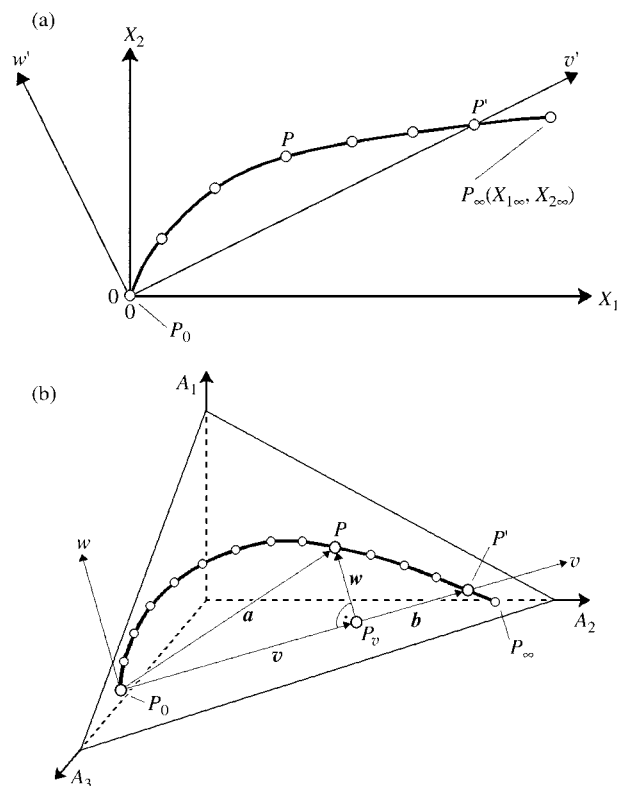


Fig. 2 (a) X_1 vs. X_2 for reactions of two independent steps ($s = 2$). The coordinate system with axes v' and w' is obtained by rotation of the system X_1 vs. X_2 around the origin. P_0 and P_∞ are the initial and end points of reactions. P (as well P') are points of the reaction system. P' may be P_∞ or may lie near to P_∞ ($P' = P$). (b) A_1 vs. A_2 vs. A_3 . The points of a reaction system consisting of two linearly independent reactions lie, generally, on a plane. P_0 and P_∞ are the initial and end points of reactions. Values of P are the time dependent points (as well P'). P' may be P_∞ or may lie near to P_∞ . The line P_0P' generates the axis v . The axis w is perpendicular to v and lies in the plane of the curve (P).

obtained in the three-dimensional absorbance space which lies in a plane. The 'original' two-dimensional curve of diagram A_2 vs. A_3 (see Fig. 2(b)) can be directly constructed from the three-dimensional curve by parallel projection when the projection rays have the same direction of axis A_1 (or $-A_1$). Thus, both curves of A_2 vs. A_3 and A_1 vs. A_2 vs. A_3 can be transduced into each other by an affine transformation. The characteristic properties remain conserved, again. In analogy, a curve on a plane in four-dimensional space (A_1 vs. A_2 vs. A_3 vs. A_4) can be transduced by parallel projection into the three-dimensional space (A_1 vs. A_2 vs. A_3). The characteristic quantities of both curves are again identical. To summarize this reflection, the characteristics of the curve are preserved when the two- or n -dimensional absorbance space is evaluated (in the case of $s = 2$).

By analogy to Fig. 2(a), a coordinate system with axes v and w can be constructed which lies in the plane of the absorbance curve (see Fig. 2(b)). The axis v passes through points P_0 and P' . The axis w is orientated perpendicularly to v and runs through P_0 (in principal, an orthogonal coordinate system is not necessary here). The coordinates of P can be characterized by means of axes v and w . To establish the corresponding equations for P the following vectors are introduced:

$$\Delta \mathbf{A} = \mathbf{a} = \mathbf{P}_0 \mathbf{P} = \begin{pmatrix} a_1 \\ \vdots \\ a_n \end{pmatrix} = \begin{pmatrix} A_{1P} - A_{10} \\ \vdots \\ A_{nP} - A_{n0} \end{pmatrix}, \quad (20a)$$

$$\mathbf{b} = \mathbf{P}_0 \mathbf{P}' = \begin{pmatrix} b_1 \\ \vdots \\ b_n \end{pmatrix} = \begin{pmatrix} A_{1P'} - A_{10} \\ \vdots \\ A_{nP'} - A_{n0} \end{pmatrix}, \quad (20b)$$

Table 2 Aminolysis of Boc-gly-ONP (9×10^{-5} M) and n -butylamine (9×10^{-5} M) in acetonitrile (temperature 25.0 °C; see ref. 1); evaluation according to eqns. (4a) and (4b). Mean value of k : $2.83 \text{ M}^{-1} \text{ s}^{-1}$. Evaluation according to eqns. (18a) and (18b) using the six-dimensional Mauser space (A_{320} vs. A_{310} vs. A_{270} vs. A_{265} vs. A_{260} vs. A_{230}), $k_1 = 2.82 \text{ M}^{-1} \text{ s}^{-1}$

λ/nm	320	310	270	265	260	230
$k_1/\text{M}^{-1} \text{ s}^{-1}$	2.8(0)	2.7(8)	2.8(7)	2.8(5)	2.8(3)	2.8(6)

$$\mathbf{v} = \mathbf{P}_0 \mathbf{P}_v = \begin{pmatrix} v_1 \\ \vdots \\ v_n \end{pmatrix} \quad (20c)$$

and

$$\mathbf{w} = \mathbf{P}_v \mathbf{P} = \begin{pmatrix} w_1 \\ \vdots \\ w_n \end{pmatrix} \quad (20d)$$

The orthogonal projection of \mathbf{a} onto the axis \mathbf{v} leads to the vector \mathbf{v} and its endpoint P_v ($\mathbf{v} = \mathbf{P}_0 \mathbf{P}_v$, see Fig. 2(b)); \mathbf{w} is the direction vector $\mathbf{P}_v \mathbf{P}$. The lengths of \mathbf{v} and \mathbf{w} are the required quantities which can be obtained by basic vector algebra^{7,8}

$$|\mathbf{v}| = v = \alpha (b_1^2 + \dots + b_n^2)^{1/2}$$

with

$$\alpha = \frac{a_1 b_1 + \dots + a_n b_n}{b_1^2 + \dots + b_n^2} \quad (21a)$$

and

$$|\mathbf{w}| = w = [(a_1 - v_1)^2 + \dots + (a_n - v_n)^2]^{1/2}$$

with

$$v_1 = \alpha b_1, \dots, v_n = \alpha b_n \quad (21b)$$

The quantities v and w can replace the role of A_1 and A_2 in eqns. (6a) and (6b) and of ΔA_1 and ΔA_2 in eqns. (8a) and (8b). When the same symbols (z_{ij}) are used for the coefficients as in eqns. (6a) and (6b), it is true for the system (5a) and (5b) that

$$d\mathbf{v} = \mathbf{z}_0 dt + \mathbf{Z} \mathbf{v} dt \quad (22a)$$

with

$$d\mathbf{v} = \begin{pmatrix} dv \\ dw \end{pmatrix}, \mathbf{z}_0 = \begin{pmatrix} z_{10} \\ z_{20} \end{pmatrix}, \mathbf{Z} = \begin{pmatrix} z_{11} & z_{12} \\ z_{21} & z_{22} \end{pmatrix}, \mathbf{v} = \begin{pmatrix} v \\ w \end{pmatrix} \quad (22b)$$

The coefficients z_{ij} of \mathbf{Z} generate a determinant (D) and trace (S) in analogy to eqns. (6c) and (6d) from which k_1 and k_2 can be computed for system (5a) and (5b) according to eqn. (6e) (even if the functional expressions of z_{ij} in eqns. (22a) and (22b) are not identical with those in eqns. (6a) and (6b)). The eigenvalues of \mathbf{Z} for system (5a) and (5b) are $r_1 = -k_1$ and $r_2 = -k_2$.

Instead of eqns. (8a) and (8b) it holds that (using the same symbols z_{ij} and y_{ij} for the coefficients)

$$d\mathbf{v} = \mathbf{z}_0 dt + \mathbf{Z} \mathbf{v} dt + \mathbf{Y} \mathbf{v}^2 dt \quad (23a)$$

with

$$d\mathbf{v} = \begin{pmatrix} dv \\ dw \end{pmatrix}, \mathbf{z}_0 = \begin{pmatrix} z_{10} \\ z_{20} \end{pmatrix}, \mathbf{Z} = \begin{pmatrix} z_{11} & z_{12} \\ z_{21} & z_{22} \end{pmatrix},$$

$$\mathbf{v} = \begin{pmatrix} v \\ w \end{pmatrix}, \mathbf{Y} = \begin{pmatrix} y_{11} & y_{12} & y_{13} \\ y_{21} & y_{22} & y_{23} \end{pmatrix}$$

and

$$\mathbf{v}^2 = \begin{pmatrix} v^2 \\ w^2 \end{pmatrix} \quad (23b)$$

By means of z_{ij} from \mathbf{Z} the quantities D and S can be established, in analogy to eqns. (8d) and (8e) for system (7a) and (7b), leading to k_1 and k_2 with the help of eqn. (8f) (even if the coefficients z_{ij} and y_{ij} in eqns. (23a) and (23b) are not identical with those of eqns. (8a) and (8b)).

4.2 Practical examples ($s = 2$)

4.2.1 First order reactions. The simultaneous hydrolyses of Boc-gly-ONP and oNPA (*o*-nitrophenyl acetate) have been studied in detail in refs. 1, 3 and 5 using a 0.1 M borax buffer (pH = 8.7; temperature 25.0 °C) (Scheme 3). ADQ diagrams can be plotted to determine the number (s) of linearly independent reactions.^{1,2} When straight lines are obtained for different wavelength combinations the case $s = 2$ is realized obeying, generally, the following functional relationship ($\lambda = 1,2,3$)^{1,2}

$$\frac{\Delta A_1}{\Delta A_2} = \alpha_1 + \alpha_2 \frac{\Delta A_3}{\Delta A_2} \quad (24a)$$

with

$$\Delta A_\lambda = A_\lambda - A_{\lambda 0} \quad (24b)$$

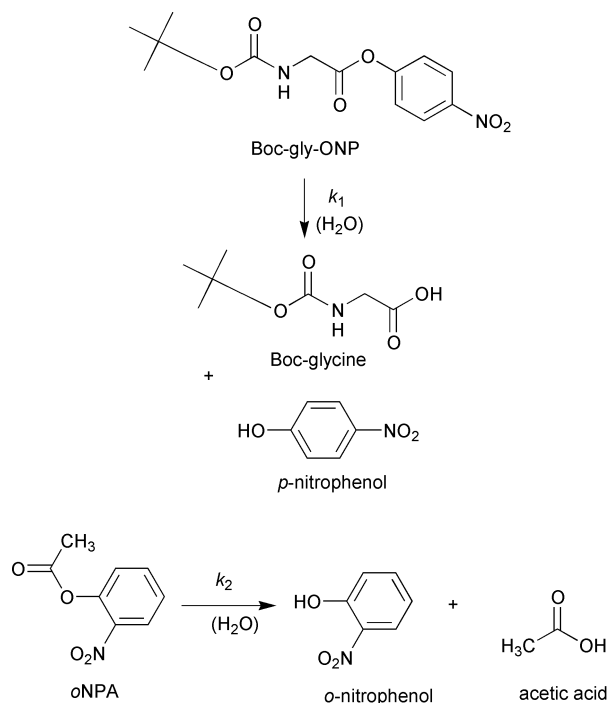
Rearrangement of this equation leads to

$$A_1 = \alpha_1 A_2 + \alpha_2 A_3 - \alpha_1 A_{20} - \alpha_2 A_{30} + A_{10} \quad (25)$$

The last equation represents a plane on which the three-dimensional curve lies in a diagram of A_1 vs. A_2 vs. A_3 . The corresponding plot for Scheme 3 is shown in Fig. 3(a). Obviously, the curve lies on a plane. To confirm this assumption, the coordinate system is rotated until the edge of the plane is seen. From this viewpoint, the curve represents a straight line (Fig. 3(b)). This procedure demonstrates that 3D plots can be also used directly instead of two-dimensional ADQ diagrams. The advantage of such 3D plots is that problems are avoided here which can appear in ADQ diagrams (strongly scattering points and artefacts, see for example, refs. 1 and 2).

The reaction system of Scheme 3 can be described by eqns. (5a) and (5b). The results of evaluation according to eqns. (6a)–(6e) are given in Table 3.

The quantities v and w were determined in the diagram A_{420} vs. A_{380} vs. A_{290} vs. A_{260} as demonstrated in Fig. 2(b). The plot v vs. w obtained is shown in Fig. 4. Evaluation of the time dependence data of v and w according to eqns. (22a), (22b), (6c)–(6e) leads to nearly 'ideal' mean values of k_1 and k_2 which can be computed from all possible two-wavelength combinations as shown in Table 3. The coefficients of eqn. (22a) showed an error which was less than 0.5%.



Scheme 3

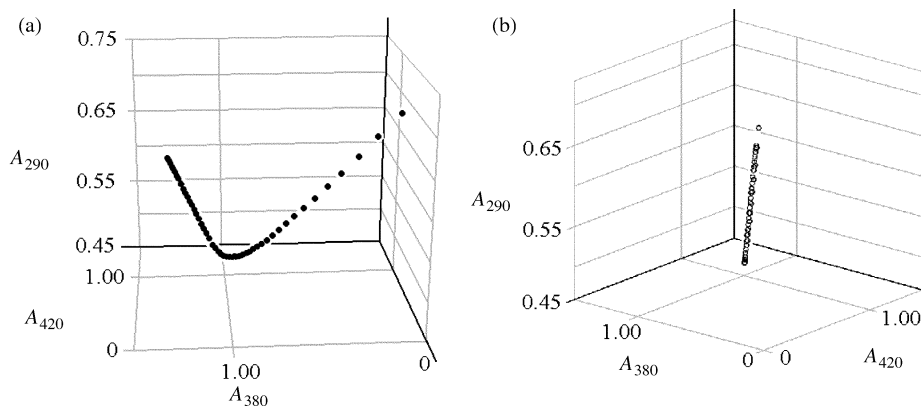


Fig. 3 (a) A_{420} vs. A_{380} vs. A_{290} for Scheme 3 (the indices indicate the wavelengths used). (b) Rotation of part (a). The curve lies on a plane and is viewed along the edge of this plane. The result is a straight line indicating the case $s = 2$.

Table 3 Spontaneous hydrolysis of Boc-gly-ONP and oNPA in 0.1 M borax buffer (pH 8.7; temperature 25.0 °C; see refs. 1, 3 and 5); evaluation according to eqns. (6a)–(6e). Mean value of $k_1 = 1.73 \times 10^{-4} \text{ s}^{-1}$. Mean value of $k_2 = 2.07 \times 10^{-3} \text{ s}^{-1}$. Evaluation of diagram A_{420} vs. A_{380} vs. A_{290} vs. A_{260} according to eqns. (22a), (22b) and (6c)–(6e), $k_1 = 1.7(3) \times 10^{-4} \text{ s}^{-1}$ and $k_2 = 2.0(7) \times 10^{-3} \text{ s}^{-1}$

λ_1/λ_2	420/380	420/290	420/260	380/290	380/260	290/260
$k_1 \times 10^4/\text{s}^{-1}$	1.6(7)	1.7(3)	1.7(4)	1.7(5)	1.7(2)	1.7(4)
$k_2 \times 10^3/\text{s}^{-1}$	2.0(0)	2.0(9)	2.1(2)	2.0(7)	2.0(5)	2.0(8)

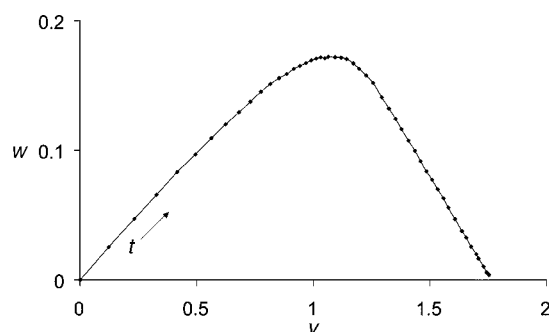


Fig. 4 Plot w vs. v for Scheme 3. The coordinates v and w have been obtained from a plot of A_{420} vs. A_{380} vs. A_{290} vs. A_{260} (as explained in Fig. 2(b)).

4.2.2 Second order reactions. Boc-gly-ONP and oNPA react with *n*-butylamine in acetonitrile as solvent according to the mechanism^{1,9}



The components are: A = *n*-butylamine; B = Boc-gly-ONP; C = *t*-Boc-glycine-*n*-butylamide; D = *p*-nitrophenol; E = oNPA; F = *N*-acetyl-*n*-butylamide; G = *o*-nitrophenol.

The quantities v and w were determined by means of a plot of A_{370} vs. A_{350} vs. A_{330} as demonstrated in Fig. 2(b). The evaluation according to eqns. (23a) and (23b) was carried out

Table 4 Aminolysis of Boc-gly-ONP (1×10^{-4} M) and oNPA (2×10^{-4} M) with *n*-butylamine (6×10^{-4} M) in acetonitrile as solvent (25.0 °C); the reaction spectra were recorded with a diode array spectrometer (Hewlett Packard 8453, Agilent Technologies); evaluation according to eqns. (8a)–(8i). Evaluation of a plot of A_{370} vs. A_{350} vs. A_{330} according to eqns. (23a), (23b) and (8d)–(8i), $k_1 = 2.8(0) \text{ M}^{-1} \text{ s}^{-1}$ and $k_2 = 0.3(6) \text{ M}^{-1} \text{ s}^{-1}$

λ_1/λ_2	370/350	370/330	350/330
$k_1/\text{M}^{-1} \text{ s}^{-1}$	(2.1)	2.7(9)	2.7(5)
$k_2/\text{M}^{-1} \text{ s}^{-1}$	0.3(9)	0.3(3)	0.3(5)

with the ‘singular value decomposition method’ (SVD).^{10,11} The coefficients z_{ij} of Z (see eqn. (23a)) lead to the required rate constants k_1 and k_2 according to eqns. (8d)–(8i) (the tolerance for z_{ij} was $5E-5$). The results are shown in Table 4 and compared with those obtained by the classical ‘two-wavelengths evaluations’. Analysis of the individual reactions ((7a) and (7b)) measured separately led to the values^{1,9} $k_1 = 2.86 \text{ M}^{-1} \text{ s}^{-1}$ and $k_2 = 0.35 \text{ M}^{-1} \text{ s}^{-1}$.

5 General discussion

In general, the kinetic analysis of chemical reactions is carried out by establishing the equations which model the presumed mechanism. A series of linear and non-linear procedures have been developed for the analysis of experimental data.^{12–20} Great mathematical efforts were made to develop criteria for the identifiability and distinguishability of such systems.^{21–24} Dynamical systems which are described by linear and non-linear differential equations are of special interest here.^{25–33}

Knowledge of the linearly independent reaction steps (s) establishing a mechanism is important for kinetic analysis. The same modern multivariate procedures for analyzing unknown mixtures can also be applied here.^{34–37} First-order multivariate methods have been successfully applied (such as partial least-squares regression (PLSR) methods and the principal component regression (PCR) method).^{38–40} Neither the reaction order nor the rate constants involved have to be known.

The determination of the number s can also be obtained by geometric analysis of the Mauser space as demonstrated in Figs. 1(b) and 3(b). This procedure is significant and needs no complex mathematical operations. The judgement of graphical results is both simple and meaningful. Additionally, the information in the n -dimensional Mauser diagram can be condensed geometrically to principal quantities (v , w) that describe spectroscopically the reaction system. These quantities can be evaluated kinetically on the basis of differential and integrated equations^{25–33} or by the method of formal integration as shown here.

Systems consisting of first and/or second order reactions can be characterized by Jacobian matrices.^{1,2,6,9,41} Their eigenvalues are identical to those of the corresponding matrices Z (compare equations (6a), (8a), (22a) and (23a)). The matrix Z can be obtained from the corresponding Jacobian matrix by a similarity transformation.^{1,2,6,9,41} Similar

matrices have the same eigenvalues. Reversed, the matrix Z which can be obtained spectroscopically leads to the eigenvalues of the Jacobian matrix which are searched for in general.

According to theorem 2 given in refs. 1 and 41 two strictly linear reaction systems whose Jacobian matrices have the same rank can not be distinguished from each other by purely spectroscopic means. And according to theorem 3^{1,41} thermally controlled reaction systems that consist of s linearly independent reaction steps—one step of which is at least a reaction of second order—can not be distinguished from each other by purely spectroscopic means if their eigenvalues have the same functional dependence on the initial concentrations. Because of these two theorems evaluation of the n -dimensional Mauser space using the method described here is generally applicable to cases $s = 1$ and $s = 2$ for linear and non-linear reaction systems. Thus, for example, the following systems can be evaluated here,

for $s = 1$: $A \rightleftharpoons B$

$A \rightarrow B, A \rightarrow C$

$A + B \rightleftharpoons C$

and for $s = 2$: $A \rightleftharpoons B \rightleftharpoons C$

$A \rightarrow B, C \rightleftharpoons D$

$A + B \rightleftharpoons C + D, E \rightarrow F + D$

$A \rightleftharpoons B, B + C \rightleftharpoons D$

The characteristic equations developed here are also true for these systems (compare eqns. (17a), (18a), (22a), (22b), (23a) and (23b)). However, the eigenvalues of the corresponding system, instead of the rate constants, are then obtained by kinetic analysis.

Kinetic evaluation of Scheme 3 represents a procedure which is applicable to many linear reactions such as, for example, $A \rightarrow B \rightarrow C$ ($s = 2$). As well, system (7a) and (7b) is representative of about 100 mechanisms including second order reactions ($s = 2$).^{1,2,6,9,41} The practical examples chosen here are appropriate to check the new evaluation procedure.

Comparison of efficiency between the formal integration and more classic evaluation procedures has demonstrated the preferred position of formal integration.¹ Consequently, the method presented here was only compared with the results obtained earlier by formal integration. As shown here, the results can even be improved when the n -dimensional Mauser space is used in combination with formal integration. The criteria for selecting appropriate wavelengths to establish the Mauser space are essentially the same as those for the construction of the Mauser diagrams.^{1,2}

In the special case of linear reactions, a reduction of the system is possible on the basis of the concept of parallel projection ($s = 2 \rightarrow s = 1$,⁵ $s = 3 \rightarrow s = 2 \rightarrow s = 1$ ⁴). The concept of parallel projection is also true for Mauser space. Thus, reaction systems with poor spectroscopic properties may be more significantly analyzed by the combination of the Mauser space with the concept of parallel projection.

The method of formal integration, according to H. Mauser,^{1,2} enables the solution of kinetic problems on the basis of linear regression even in the case of second order reactions. For example, the (integral) concentration equations of the reaction system $A + B \rightarrow C \rightarrow D$ are based on the beta function.^{4,2} The application of eqn. (23a), which is true for about 100 reaction mechanisms, is independent of such complex functions. Thus, the simultaneous evaluation of absorbances from several wavelengths possesses a potential which has not yet been exhausted.

6 Conclusions

Mauser space is a powerful tool in the kinetic analysis of ther-

mally controlled reaction systems (as well as of quasi-linear photoreactions).

This work was kindly supported by the Deutsche Forschungsgemeinschaft (DFG, Bonn, Germany; project Po222/8-1). We thank Dr. Gänzle, Institute of Technical Microbiology of the Technical University München (Freising-Weihenstephan, Germany), for the construction of Figs. 1(a), 1(b), 3(a) and 3(b). We thank Dipl. mat. Schleip (Lehrstuhl für Fluidmechanik und Prozeßautomation, TU München) for helpful discussions.

References

- 1 J. Polster, *Reaktionskinetische Auswertung Spektroskopischer Meßdaten*, Vieweg-Verlag, Wiesbaden, 1995.
- 2 H. Mauser and G. Gauglitz, *Photokinetics, Theoretical Fundamentals and Applications*, Elsevier, Amsterdam, 1998.
- 3 J. Polster, *Ber. Bunsenges. Phys. Chem.*, 1998, **102**, 1496.
- 4 J. Polster, *Chem. Phys.*, 1999, **240**, 331.
- 5 J. Polster, *Phys. Chem. Chem. Phys.*, 1999, **1**, 4791.
- 6 H. Mauser, *Z. Naturforsch., Teil A*, 1987, **42**, 713.
- 7 M. M. Lipschutz, *Differential Geometry*, Schaum's Outline Series, McGraw-Hill, New York, 1969.
- 8 H. Netz (with J. Rast), *Formeln der Mathematik*, Carl Hanser Verlag, München, 1983.
- 9 J. Polster and H. Mauser, *Talanta*, 1992, **39**, 1355.
- 10 J. H. Wilkinson, in *Numerical Software—Needs and Availability*, Academic Press, New York, 1978.
- 11 W. H. Press, B. R. Flannery, S. A. Teukolsky and W. T. Vetterling, *Numerical Recipes in PASCAL*, Cambridge University Press, Cambridge, 1989.
- 12 F. J. Kézdy, J. Jaz and A. Bruylants, *Bull. Soc. Chim. Belg.*, 1958, **67**, 687.
- 13 E. S. Swinbourne, *J. Chem. Soc.*, 1960, **473**, 2371.
- 14 S. W. Benson, *The Foundations of Chemical Kinetics*, McGraw-Hill, New York, 1960.
- 15 K. J. Laidler, *Reaction Kinetics*, Pergamon Press, Oxford, 1963, vols. I and II.
- 16 A. A. Frost and R. G. Pearson, *Kinetik und Mechanismus Homogener Reaktionen*, Verlag Chemie, Weinheim, 1973.
- 17 K. Schwetlick, H. Dunken, G. Pretzschner, K. Scherzer and H.-J. Tieler, *Chemische Kinetik*, Fachstudium Chemie, Lehrbuch 6, Verlag Chemie, Weinheim, 1974.
- 18 H. Strehlow and W. Knoche, *Fundamentals of Chemical Relaxation*, Verlag Chemie, Weinheim, 1977.
- 19 H.-H. Perkampus, *UV-VIS-Spektroskopie und ihre Anwendungen*, Springer-Verlag, Berlin, 1986.
- 20 K. A. Connors, *Chemical Kinetics*, VCH, Weinheim, 1990.
- 21 E. Walter, *Identifiability of State Space Models*, Springer, Berlin, 1982.
- 22 J. A. Jaquez, *Math. Comput. Simul.*, 1982, **24**, 452.
- 23 J. Eisenfeld, *Math. Biosci.*, 1986, **79**, 209.
- 24 J. Delforge, *Math. Biosci.*, 1986, **81**, 127.
- 25 J. Benz, J. Polster, R. Bär and G. Gauglitz, *Comput. Chem.*, 1987, **11**, 41.
- 26 S. Vajda and H. Rabitz, *J. Phys. Chem.*, 1988, **92**, 701.
- 27 S. Vajda and H. Rabitz, *J. Phys. Chem.*, 1994, **98**, 5265.
- 28 G. Li and H. Rabitz, *J. Phys. Chem.*, 1996, **105**, 4065.
- 29 G. Li and H. Rabitz, *Chem. Eng. Sci.*, 1997, **52**, 4317.
- 30 G. Li and H. Rabitz, *J. Chem. Phys.*, 1997, **107**, 2845.
- 31 A. Molski and N. Boens, *J. Chem. Phys.*, 1999, **110**, 1623.
- 32 J. Saurina, S. Hernandez-Carsson, R. Tauler and A. Izquierdo-Ridors, *J. Chemomet.*, 1998, **12**, 183.
- 33 A. Molski and N. Boens, *J. Chem. Phys.*, 1999, **110**, 1628.
- 34 S. Wold, H. Martens and H. Wold, in *Matrix Pencils*, ed. A. Ruhe and B. Kagstrom, Lecture Notes in Mathematics, 1994, p. 286.
- 35 D. L. Massart, B. G. M. Vandeginste, S. N. Deming, Y. Michotte and L. Kaufman, *Chemometrics: a Textbook*, Elsevier, Amsterdam, 1988.
- 36 H. Martens and T. Naes, *Multivariate Calibration*, Wiley, Chichester, 1989.
- 37 A. Eberkali, J. Nygren and M. Kubista, *Anal. Chim. Acta*, 1999, **379**, 143.
- 38 M. Blanco, J. Coello, H. Ituringa, S. Maspoch and J. Riba, *Anal. Chem.*, 1994, **66**, 2905.
- 39 Z. Gu and X. Wang, *Talanta*, 1995, **42**, 205.
- 40 Y. Xie, J. J. Baeza-Baeza and G. Ramis-Ramos, *Chemom. Intell. Lab. Syst.*, 1995, **27**, 211.
- 41 H. Mauser and J. Polster, *Z. Naturforsch., Teil A*, 1995, **50**, 1031.
- 42 T. Kelen, *Phys. Chem. N. F.*, 1968, **60**, 191.